

Article

An Evaluation of Choroidal and Retinal Nerve Fiber Layer Thicknesses Using SD-OCT in Children with Childhood IgA Vasculitis

Ali Simsek ^{1,*}  and Mehmet Tekin ² 

¹ Department of Ophthalmology, School of Medicine, Adiyaman University, Kahta Street, Adiyaman 02000, Turkey

² Department of Pediatrics, School of Medicine, Adiyaman University, Adiyaman 02000, Turkey; drmehmetekin@hotmail.com

* Correspondence: alisimsek1980@gmail.com; Tel.: +90-530-222-77-60; Fax: +90-414-318-31-92-11

Abstract: Background: We aimed to evaluate choroidal and retinal nerve fiber layer (RNFL) thicknesses in children undergoing the childhood IgA vasculitis (IgAV). Methods: Fifty-two patients with IgAV aged 1–6 years and 54 healthy children were included. Cases' age, sex, erythrocyte sedimentation rate (ESR), C-reactive protein (CRP), RNFL thicknesses, and choroidal thickness values were recorded. Results: Median foveal center choroidal thickness was 374.0 μm (315.0 to 452.0 μm) in the IgAV group and 349.5 μm (285.0 to 442.0 μm) in the control group ($p = 0.001$). Median average RNFL thickness was 110.0 μm (91.0 to 134.0 μm) in the IgAV group and 104.0 μm (89.0 to 117.0 μm) in the control group ($p < 0.001$). Choroidal and RNFL thicknesses were significantly greater in all quadrants in the IgAV group than in the control group. No correlation was determined between ESR or CRP and foveal center choroidal and average RNFL thicknesses. Conclusions: Our findings show that choroidal and RNFL thicknesses increased significantly in children undergoing childhood IgA vasculitis compared to the healthy control group. These findings show that the choroid and RNFL are also affected by the inflammatory process in IgAV, which is a systemic vasculitis. We think that the choroidal and RNFL thicknesses can be used as a biomarker for childhood IgAV.

Keywords: childhood; choroid; IgA vasculitis; retinal nerve fiber layer



Citation: Simsek, A.; Tekin, M. An Evaluation of Choroidal and Retinal Nerve Fiber Layer Thicknesses Using SD-OCT in Children with Childhood IgA Vasculitis. *Diagnostics* **2022**, *12*, 901. <https://doi.org/10.3390/diagnostics12040901>

Academic Editors: Louis Arnould, Ryo Kawasaki, Fabrice Meriaudeau and João Barbosa-Breda

Received: 9 February 2022

Accepted: 8 March 2022

Published: 5 April 2022

Publisher's Note: MDPI stays neutral with regard to jurisdictional claims in published maps and institutional affiliations.



Copyright: © 2022 by the authors. Licensee MDPI, Basel, Switzerland. This article is an open access article distributed under the terms and conditions of the Creative Commons Attribution (CC BY) license (<https://creativecommons.org/licenses/by/4.0/>).

1. Introduction

Childhood Immunoglobulin A vasculitis (IgAV), formerly called Henoch–Schönlein purpura, is the most common vasculitis in children. The majority of cases are aged under 10, and there is no gender bias. This systematic, non-granulomatous vasculitis is characterized by the accumulation of immune complexes containing immunoglobulin A in the walls of the small vessels (arterioles, capillary vessels, and venules). Due to its systemic nature, multiorgan involvement is seen in cases of IgAV [1]. Diagnosis of IgAV is based on clinical findings in case of at least one of abdominal pain/gastrointestinal bleeding, arthralgia/arthritis, or hematuria/proteinuria accompanying palpable purpura, particularly in the lower extremities (Figure 1) [2].

Uveitis is one of the main clinical findings in Behçet's disease, another systemic vasculitis, and choroidal thickening has been reported in patients with uveitis [3,4]. However, choroidal thinning has been reported in non-uveitis Behçet's disease, and subclinical choroidal involvement must not be overlooked [5]. Increased subfoveal choroidal thickness has also been reported in patients with polyarteritis nodosa, another systemic vasculitis [6].



Figure 1. A child with palpable purpura in the lower extremities.

The choroid is a densely vascularized structure consisting of a network of capillaries and larger vessels with several functions, including supplying oxygen and other nutrients to the outer layers of the retina and retinal pigment epithelium, removing metabolic waste products from the outer retina, and temperature regulation [7]. The layers of the retina can be examined in detail using spectral domain optical coherence tomography (SD-OCT), and the choroid, a vascular bed nourishing the retina, can be evaluated using enhanced depth imaging optical coherence tomography (EDI-OCT) [8]. Currently, SD-OCT is the gold standard non-invasive imaging technique for the diagnosis of clinical ocular diseases such as age-related macular degeneration, diabetic retinopathy, central serous chorioretinopathy, and inherited retinal diseases. Visualization of the choroid, which plays a role in the pathogenesis of retinal diseases, was possible with the advent of SD-OCT. In addition, it is possible to measure the physical and optical parameters of the eye, including the axial length and lens thickness, with the optical biometer, which is a variant of SD-OCT [9].

In recent years, measurement of choroidal and retinal nerve fiber layer (RNFL) thicknesses with SD-OCT has been suggested as an inflammatory marker for different systemic diseases with vascular involvement, such as lupus, familial Mediterranean fever, and Behçet's disease [10]. Despite being a systemic vasculitis, to the best of our knowledge, no previous studies have examined choroidal and RNFL thicknesses in patients with IgAV. The aim of this study is to determine whether choroidal and RNFL thicknesses change in childhood IgAV and to determine whether these thicknesses can be used as an inflammatory marker in IgAV.

2. Materials and Methods

2.1. Study Design

This prospective cross-sectional study was performed between 1 September 2015 and 31 August 2019 at the Adiyaman University School of Medicine ophthalmology and pediatric clinics, Turkey. Approval for the study was granted by the Adiyaman University Medical Faculty Non-Interventional Ethical Committee (No. 2015/05-15). Procedures at all stages of the study were carried out in compliance with the principles of the Declaration of Helsinki. Informed consent forms were received from all participants or their parents before the study commenced.

Fifty-two patients with IgAV aged one to six years and fifty-four healthy children were included in the study. Diagnosis of IgAV was based on at least one of abdominal pain/gastrointestinal bleeding, arthralgia/arthritis, or hematuria/proteinuria findings accompanying palpable purpura in the lower extremities. Healthy children selected from among individuals similar to the IgAV group in terms of age and sex and presenting for routine health checks were enrolled in the control group. Patients with accompanying thrombocytopenia, anemia, malaria, syphilis, bleeding or clotting disorders, acute kidney failure (reduced glomerular filtration rate (GFR): <80 mL/min/1.73 m²), massive proteinuria (>40 mg/m²/day) or sepsis/disseminated intravascular coagulation, medical histories of systemic lupus erythematosus, polyarteritis nodosa, coagulation disorder, diabetes mellitus, renal disease, smoking, drinking, immunosuppressive/cytotoxic drug use, contact lens use, ocular trauma, keratoconus, glaucoma, topical drug use, or eye surgery, or with amblyopia, strabismus, myopia, hypermetropia, or with an astigmatic refractive error exceeding ± 1.0 D at ocular examination were excluded from the study. Choroidal thickness is influenced by a number of factors including age, gender, axial length, retinal thickness, and intraocular pressure (IOP) [11,12]. Similarly, RNFL thickness is influenced by age, axial length, and spherical equivalent [13]. Therefore, the patient and the control groups were selected from cases matched in terms of age, gender, refractive error, and axial length.

Ophthalmological Examinations

Eye examinations were performed in the first 48 h following diagnosis of IgAV. Ophthalmological examination including IOP, refractive error, split-lamp biomicroscopy, and visual acuity measurement and dilated fundus examination were performed in all cases. Best visual acuity values (as measured on a Snellen chart, decimal fraction) were recorded. Central corneal thickness (CCT) and axial length were measured using an optical biometer (Lenstar LS 900; Haag Streit AG, Koeniz, Switzerland). The RNFL and the choroid were visualized in non-dilated pupils using SD-OCT (Spectralis; Heidelberg Engineering, Heidelberg, Germany). The scan quality ranged from no signal (0) to excellent (40), and only high-quality images (a well-focused optic disc with a signal strength >20 Db and centered) were selected. The variation in the accuracy of ranging (length measurement) expected from using a different OCT machine is typically caused by the changes in the calibration and image reconstruction algorithm adopted for various OCT/biometer machines [14]. All children were examined for choroidal thickness at the same time period between 8:00 a.m. and 10:00 a.m. to avoid diurnal variations [15]. Right eye values were used for statistical analyses. To improve the visualization of the choroid, the instrument's enhanced depth imaging mode was used in combination with automatic real-time eye tracking and frame averaging. The wavelength of the OCT instrument was 870 nm, with an axial resolution of 5 μ m and a scanning speed of 40,000 A-scans per second. Each radial OCT image was the average of 30 B-scans. [16]. Each subject was imaged by both ophthalmologists (A.S. and A.A.Y.) who were blinded to the clinical information of the examined eyes, and the two values, captured by two different ophthalmologists, were averaged for analysis. Inter-examiner reproducibility of all manual measurements was evaluated by the intraclass correlation coefficient (ICC) so that values of greater than 0.80 were accepted as good agreement. Choroidal thickness was defined as the distance between the hyper reflective line and the outer retinal pigment epithelium line behind the large-sized choroidal vessel layers at the scleral interface. We manually measured the thicknesses at seven different points: at the foveal center and within the horizontal, temporal, and nasal quadrants at 500- μ m intervals as far as 1500 μ m from the foveal center. RNFL thickness was defined from the optic nerve head scan. A volumetric scanning protocol was used, imaging a 15 by 15 region surrounding the optic nerve head (circle scan size 3.4 mm). The average RNFL thickness and those in the four quadrants were automatically calculated by the SD-OCT (superior, nasal, inferior, and temporal, 90° each).

2.2. Data Acquisition

Cases' age, sex, arterial blood pressure, complete blood count, erythrocyte sedimentation rate (ESR), C-reactive protein (CRP), creatinine, albumin, complete urine examination, urinary protein level, GFR, occult blood in stool test, IOP, visual acuity, CCT, axial length, and choroidal and RNFL thicknesses were recorded.

2.3. Statistical Analysis

Statistical Package for the Social Sciences 21.0 software (SPSS Inc., Chicago, IL, USA) was used for statistical analyses. The chi-square test was used to compare categorical variables. The Kolmogorov–Smirnov test was performed to determine whether the continuous data were normally distributed. The independent Student *t* test was used for comparison of normally distributed data, and these results were expressed as mean \pm standard deviation. Non-normally distributed data were compared with the Mann–Whitney U test and values were expressed as median (minimum to maximum). Pearson correlation analysis was applied to determine a linear relationship between CRP and ESR and choroidal and RNFL thicknesses. *p* values < 0.05 were considered statistically significant.

3. Results

Fifty-eight patients with IgAV were originally included in the study, but two were excluded due to nephrotic proteinuria secondary to IgAV, one because of development of acute kidney failure (eGFR: <80 mL/min/1.73 m²), two due to pronounced refractive error, and one because a high-quality image could not be obtained. The study thus continued with 52 patients with IgAV and 54 healthy children. Girls constituted 24 (46.2%) of the IgAV group and boys 28 (53.8%), while 25 (46.3%) of the control group were girls and 29 (53.7%) were boys. Mean ages were 7.1 \pm 2.4 years in the IgAV group and 7.8 \pm 2.3 in the control group. There was no significant difference between the groups in terms of sex or age (*p* = 0.571 and *p* = 0.154, respectively). Median CRP was 3.20 (0.01–15.30) mg/dL and median ESR 16 (5–32) mm/h in the IgAV group, compared to 0.40 (0.01–3.50) mg/dL and 7 (3–15) mm/h in the control group. CRP and ESR values were significantly higher in the IgAV group (*p* < 0.001 for both). No significant difference was determined between the groups in terms of hemoglobin, creatinine, or albumin values. No difference was also determined between the groups in terms of IOP, visual acuity, axial length, or CCT (Table 1). No cotton-wool spot, conjunctivitis, uveitis, keratitis, scleritis, episcleritis, optical neuritis, macular edema, papilledema, or retinal hemorrhage/infarct was observed in either group.

Table 1. Demographic, laboratory, and ocular characteristics of the groups.

| | IgAV Group (n = 52) | Control Group (n = 54) | <i>p</i> |
|---|------------------------|---------------------------|----------|
| Gender (F/M) # | 24/28 | 25/29 | 0.571 |
| Age (year) † | 7.1 \pm 2.4 | 7.8 \pm 2.3 | 0.154 |
| Hemoglobin (g/dL) † | 11.9 \pm 0.9 | 11.8 \pm 0.8 | 0.676 |
| CRP (mg/dL) ¶ | 3.20 (0.01–15.30) | 0.40 (0.01–3.50) | <0.001 * |
| ESR (mm/h) ¶ | 16 (5–32) | 7 (3–15) | <0.001 * |
| Creatinine (mg/dL) † | 0.60 \pm 0.18 | 0.57 \pm 0.14 | 0.390 |
| Albumin (mg/dL) † | 3.54 \pm 0.30 | 3.48 \pm 0.28 | 0.334 |
| IOP (mmHg) † | 14.2 \pm 1.3 | 13.7 \pm 1.2 | 0.054 |
| Visual acuity (Snellen chart, in decimal) † | 1.14 \pm 0.12 | 1.17 \pm 0.09 | 0.147 |
| CCT (μ m) † | 532.4 \pm 20.4 | 530.7 \pm 26.0 | 0.704 |
| Axial length (mm) † | 22.02 \pm 0.78 | 22.06 \pm 0.83 | 0.817 |

* *p* < 0.05; # Chi-square test; † Independent Student *t* test, mean \pm standard deviation; ¶ Mann–Whitney U test, median (minimum–maximum); IgAV, immunoglobulin A vasculitis; CRP, C-reactive protein; ESR, erythrocyte sedimentation rate; IOP, intraocular pressure; CCT, central corneal thickness.

Foveal center choroidal thicknesses measured using EDI-OCT were 374.0 μm (315.0 to 452.0 μm) in the IgAV group (Figure 2) and 349.5 μm (285.0 to 442.0 μm) in the control group ($p = 0.001$). Choroidal thicknesses in all quadrants in the IgAV group were significantly greater than in the control group (Table 2).

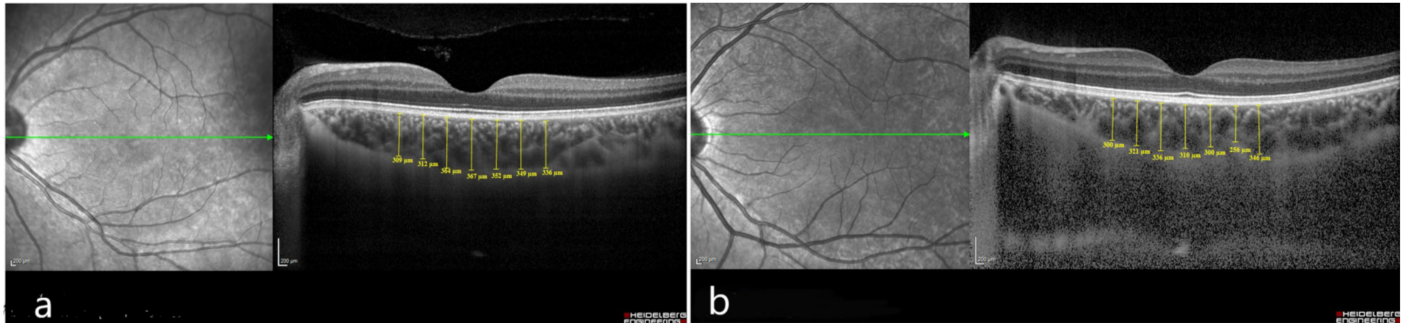


Figure 2. (a) Choroidal thickness measurements obtained by spectral-domain optical coherence tomography in a child with immunoglobulin A vasculitis. (b) Choroidal thickness measurements in a child from the control group. Images were obtained by averaging multiple B-scans from same position in both groups.

Table 2. Comparisons of Choroidal Thicknesses in the Right Eyes of Immunoglobulin A Vasculitis and Control Groups.

| | IgAV Group (n = 52) | Control Group (n = 54) | <i>p</i> |
|------------------------------|------------------------|---------------------------|----------------|
| Foveal center, μm | 374.0 (315.0–452.0) | 349.5 (285.0–442.0) | 0.001 * |
| Temporal, 1500 μm | 320.5 (290.0–400.0) | 300.0 (251.0–400.0) | 0.016 * |
| Nasal, 1500 μm | 302.5 (233.0–433.0) | 290.0 (220.0–370.0) | 0.003 * |
| Temporal, 1000 μm | 342.5 (234.0–420.0) | 319.0 (254.0–420.0) | 0.009 * |
| Nasal, 1000 μm | 324.0 (261.0–418.0) | 300.0 (231.0–398.0) | 0.002 * |
| Temporal, 500 μm | 359.0 (301.0–437.0) | 332.5 (258.0–437.0) | 0.004 * |
| Nasal, 500 μm | 345.0 (250.0–493.0) | 316.0 (245.0–410.0) | 0.003 * |

* $p < 0.05$ Mann–Whitney U test was used for comparisons and results were expressed as median (minimum to maximum) values; IgAV, immunoglobulin A vasculitis.

Median average RNFL thicknesses were 110.0 μm (92.0 to 134.0 μm) in the IgAV group (Figure 3) compared to 104.0 μm (89.0 to 117.0 μm) in the control group ($p < 0.001$). RNFL thicknesses were significantly higher in all quadrants in the IgAV group compared to the control group (Table 3).

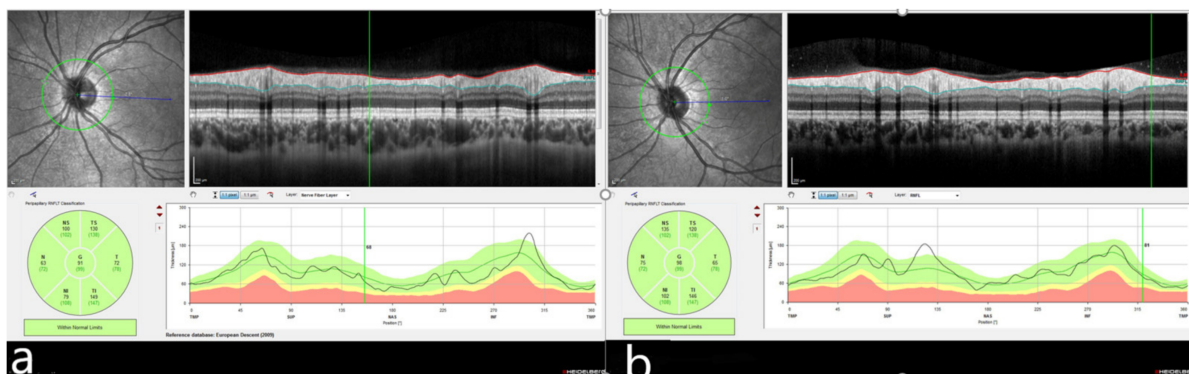


Figure 3. (a) Retinal nerve fiber layer thickness measurements obtained by spectral-domain optical coherence tomography in a child with immunoglobulin A vasculitis. (b) Retinal nerve fiber layer thickness in a child from the control group. Images were obtained by averaging multiple B-scans from the same position in both groups.

Table 3. Comparisons of Retinal Nerve Fiber Layer Thicknesses in the Right Eyes of Immunoglobulin A Vasculitis and control groups.

| | IgAV Group (n = 52) | Control Group (n = 54) | <i>p</i> |
|----------------------------|------------------------|---------------------------|----------|
| Nasal inferior RNFL, μm | 124.0 (115.0–170.0) | 113.0 (97.0–127.0) | <0.001 * |
| Nasal superior RNFL, μm | 116.0 (108.0–153.0) | 106.0 (94.0–122.0) | <0.001 * |
| Nasal RNFL, μm | 86.0 (67.0–116.0) | 75.0 (67.0–98.0) | <0.001 * |
| Temporal inferior RNFL, μm | 162.5 (135.0–189.0) | 147.0 (129.0–175.0) | <0.001 * |
| Temporal superior RNFL, μm | 149.5 (123.0–179.0) | 137.0 (115.0–165.0) | 0.001 * |
| Temporal RNFL, μm | 89.0 (70.0–117.0) | 82.5 (59.0–107.0) | 0.001 * |
| Average RNFL, μm | 110.0 (92.0–134.0) | 104.0 (89.0–117.0) | <0.001 * |

* *p* < 0.05 Mann–Whitney U test was used for comparisons and were expressed as median (minimum to maximum) values; IgAV, immunoglobulin A vasculitis; RNFL, retinal nerve fiber layer.

Pearson correlation analysis revealed no correlation between ESR and CRP and foveal center choroidal or average RNFL thicknesses (Table 4).

Table 4. Correlation between inflammation markers and choroidal and retinal fiber layer thicknesses.

| | <i>r</i> | <i>R</i> ² | Estimated Equation | 95% CI | <i>p</i> |
|----------------------|----------|-----------------------|-------------------------|------------------|----------|
| ESR-Foveal center CT | −0.12 | 1.551E−4 | $y = 3.75E2 - 0.06 * x$ | −0.213 to +0.198 | 0.930 |
| ESR-Average RNFL | 0.126 | 0.016 | $y = 1.08E2 + 0.18 * x$ | −0.203 to +0.425 | 0.372 |
| CRP-Foveal center CT | −0.013 | 1.773E−4 | $y = 3.75E2 - 0.12 * x$ | −0.282 to +0.232 | 0.925 |
| CRP-Average RNFL | −0.260 | 0.068 | $y = 1.14E2 - 0.67 * x$ | −0.463 to +0.013 | 0.062 |

Pearson correlation was used for comparison; 95% CI, confidence interval; ESR, erythrocyte sedimentation rate; CRP, C-reactive protein; CT, choroidal thickness; RNFL, retinal nerve fiber layer.

4. Discussion

The results of this study showed a significant increase in choroidal and RNFL thicknesses in patients with IgAV compared to the healthy control group of similar age and gender. Choroidal and RNFL thicknesses increased in all quadrants in the IgAV patients.

IgAV is the most common form of vasculitis in childhood. The disease causes multi-system involvement, particularly urinary, digestive, cutaneous, and locomotor. In addition to classic findings such as abdominal pain/gastrointestinal bleeding, arthralgia/arthritis, and hemorrhage/proteinuria accompanying palpable purpura in the lower extremities, the disease can also cause pathologies such as intussusception, cerebral hemorrhage, seizure, myocarditis, myositis, and pulmonary hemorrhage [1].

In IgAV, IgA immune complexes are transported through the blood and adhere to small vessel walls, then cause an oxidative burst of neutrophils and secreted enzymes, and oxygen radicals cause disruption of the vessel basement membrane, resulting in endothelial damage [17]. The choroidal vasculature is the primary source of both oxygen and nutrients to the outer retina, including the retinal pigment epithelium, photoreceptors, and, otherwise, avascular fovea [7]. This high flow system also provides primary ocular access for the circulating immune complexes, therefore, choroid is a common site of inflammation [18]. It can be hypothesized that the choroid and RNFL, neural tissue of the eye fed by the choroid, may be influenced due to circulating IgA immune complexes. Based on these observations, we examined the choroidal and RNFL thicknesses with SD-OCT in IgAV patients.

For many years, the choroid could only be evaluated by indocyanine green angiography, ultrasound, and laser Doppler flowmetry. Although these techniques are useful for determining vessel abnormalities or changes in the choroidal blood flow, it was not possible to visualize three-dimensional anatomical information about the choroid [19]. More recently, technological improvements in structural OCT have revealed important morphological and functional characteristics of the choroid in physiological and pathological conditions, including inflammatory disease. The enhanced depth imaging OCT is a noninvasive technique that provides high-resolution cross-sectional three-dimensional images of the retina and RNFL and good repeatability of choroidal thickness measurements [20].

Uveitis, keratitis, episcleritis, and optical neuritis can be seen in the vasculitic condition Behçet's disease [21,22]. Cotton-wool spots, anterior ischemic optic neuropathy, central retinal artery occlusion, posterior scleritis, and choroiditis have been reported in patients with polyarteritis nodosa [23]. Bilateral conjunctivitis, uveitis, iridocyclitis, superficial punctate keratitis, vitreous opacities, and papilledema can be seen in Kawasaki disease [24]. Optical neuritis, retinopathy, and choroidopathy have been reported in systemic lupus erythematosus [23,25]. There have also been case reports of bilateral cystoid macular edema, cotton-wool spots, and anterior ischemic optic neuropathy in patients with IgAV [26]. No cotton-wool spot, conjunctivitis, uveitis, keratitis, scleritis, episcleritis, optical neuritis, macular edema, papilledema, or retinal hemorrhage/infarct were determined in the IgAV patients in the present study.

Chung et al. [27] reported increased choroidal thicknesses and suggested that choroidal thickness can be used as an indicator of subclinical ocular inflammation and systemic inflammation in Behçet's disease. Tetikoğlu et al. [28] reported increased choroidal thicknesses in patients with rheumatoid arthritis. Baytaroğlu et al. [6] reported increased choroidal thicknesses in patients with polyarteritis nodosa and that choroidal thickness can be employed as an indicator of subclinical systemic involvement. Some authors focused on choroidal thickness as a biomarker for cardiovascular disease risk factors [29]. Arnold et al. [30] reported that longer axial length and older age are associated with thinner subfoveal choroidal thickness, but choroidal thickness was not significantly associated with sex or cardiovascular history. In the present study, choroidal thicknesses were significantly higher in all quadrants in the patients with IgAV compared to the healthy control group. The patient and the control groups were selected from cases matched in terms of age, gender, refractive error, and axial length.

Liu et al. [31] reported significant RNFL thinning in systemic lupus erythematosus, and they speculated that OCT measurements may be indicative of neurodegeneration in systemic lupus erythematosus. Tetikoğlu et al. [28] reported no significant difference between the rheumatoid arthritis and healthy group regarding RNFL. Bayram et al. [32] reported that RNFL thickness increased significantly in patients with COVID-19 disease compared to the healthy group. Arnould et al. [33] reported that decreased retinal vessels' calibers were associated with a decreased RNFL thickness in the elderly without optic neuropathy. In the present study, RNFL thicknesses were significantly higher in all quadrants in the patients with IgAV compared to the healthy control group. We hypothesized that the increased RNFL thickness may be linked to IgA immune complexes transported through the choroid.

Additionally, no correlation was found between CRP and ESR and choroidal or RNFL thicknesses in the present study.

One of the principal limitations of the present study, which is, to the best of our knowledge, the first to investigate choroidal and RNFL thicknesses in patients with IgAV, is the relatively low number of cases. In addition, it is unknown whether the increase in choroidal and RNFL thicknesses will cause clinically detectable ocular symptoms in later years.

In conclusion, our findings show that choroidal and RNFL thicknesses increased significantly in children undergoing IgAV compared to the healthy control group. These findings show that the choroid and RNFL are also affected by the inflammatory process in IgAV, which is a systemic vasculitis. We think that the choroidal and RNFL thicknesses can be used as a biomarker for childhood IgAV. It is known that IgAV can cause kidney damage in the long term, but there are no data on its effects on vision. Our findings now need to be confirmed with larger patient groups, and the long-term clinical effects of subclinical choroidal and RNFL thickness increases also need to be observed.

Author Contributions: Conceptualization: A.S. and M.T.; Data Curation: A.S. and M.T.; Formal Analysis: A.S. and M.T.; Investigation: A.S. and M.T.; Methodology: A.S. and M.T.; Project Administration: A.S.; Writing—Original Draft: M.T.; Writing—Review and Editing: A.S. and M.T. All authors have read and agreed to the published version of the manuscript.

Funding: This research received no external funding.

Institutional Review Board Statement: The study was conducted according to the guidelines of the Declaration of Helsinki and approved by the Institutional Review Board of Adiyaman University Medical Faculty Non-Interventional Ethical Committee (No. 2015/05-15 and date of approval 16 June 2015).

Informed Consent Statement: Informed consent forms were received from all participants or their parents before the study commenced.

Data Availability Statement: The data that support the findings of this study are available from the corresponding author, upon reasonable request.

Acknowledgments: The authors would like to acknowledge the support of Ali Asgar Yetkin in obtaining Spectral Domain Optical Coherence Tomography images.

Conflicts of Interest: The authors report no conflict of interest.

References

1. Trnka, P. Henoch–Schönlein Purpura in Children. *J. Paediatr. Child Health* **2013**, *49*, 995–1003. [[CrossRef](#)]
2. Ozen, S.; Pistorio, A.; Iusan, S.M.; Bakkaloglu, A.; Herlin, T.; Brik, R.; Buoncompagni, A.; Lazar, C.; Bilge, I.; Uziel, Y.; et al. EULAR/PRINTO/PRES Criteria for Henoch–Schönlein Purpura, Childhood Polyarteritis Nodosa, Childhood Wegener Granulomatosis and Childhood Takayasu Arteritis: Ankara 2008. Part II: Final Classification Criteria. *Ann. Rheum. Dis* **2010**, *69*, 798–806. [[CrossRef](#)] [[PubMed](#)]
3. Bulur, I.; Onder, M. Behcet Disease: New Aspects. *Clin. Dermatol.* **2017**, *35*, 421–434. [[CrossRef](#)] [[PubMed](#)]
4. Ishikawa, S.; Taguchi, M.; Muraoka, T.; Sakurai, Y.; Kanda, T.; Takeuchi, M. Changes in Subfoveal Choroidal Thickness Associated with Uveitis Activity in Patients with Behçet’s Disease. *Br. J. Ophthalmol.* **2014**, *98*, 1508–1513. [[CrossRef](#)] [[PubMed](#)]
5. Mittal, A.; Velaga, S.B.; Falavarjani, K.G.; Nittala, M.G.; Sadda, S.R. Choroidal Thickness in Non-Ocular Behçet’s Disease—A Spectral-Domain OCT Study. *J. Curr. Ophthalmol.* **2017**, *29*, 210–213. [[CrossRef](#)] [[PubMed](#)]
6. Baytaroglu, A.; Kadayifçilar, S.; Ağin, A.; Deliktaş, Ö.; Demir, S.; Bilginer, Y.; Karakaya, J.; Özen, S.; Eldem, B. Choroidal Vascularity Index as A Biomarker of Systemic Inflammation in Childhood Polyarteritis Nodosa and Adenosine Deaminase-2 Deficiency. *Pediatr. Rheumatol. Online J.* **2020**, *18*, 29. [[CrossRef](#)] [[PubMed](#)]
7. Borrelli, E.; Sarraf, D.; Freund, K.B.; Sadda, S.R. OCT Angiography and Evaluation of the Choroid and Choroidal Vascular Disorders. *Prog. Retin. Eye Res.* **2018**, *67*, 30–55. [[CrossRef](#)] [[PubMed](#)]
8. Hassenstein, A.; Meyer, C.H. Clinical Use and Research Applications of Heidelberg Retinal Angiography and Spectral-Domain Optical Coherence Tomography—A Review. *Clin. Exp. Ophthalmol.* **2009**, *37*, 130–143. [[CrossRef](#)]
9. Adhi, M.; Duker, J.S. Optical coherence tomography—Current and future applications. *Curr. Opin. Ophthalmol.* **2013**, *24*, 213–221. [[CrossRef](#)] [[PubMed](#)]
10. Steiner, M.; Esteban-Ortega, M.; Muñoz-Fernández, S. Choroidal and retinal thickness in systemic autoimmune and inflammatory diseases: A review. *Surv. Ophthalmol.* **2019**, *64*, 757–769. [[CrossRef](#)]
11. Prousalis, E.; Dastiridou, A.; Ziakas, N.; Androudi, S.; Mataftsi, A. Choroidal thickness and ocular growth in childhood. *Surv. Ophthalmol.* **2021**, *66*, 261–275. [[CrossRef](#)]
12. Barteselli, G.; Chhablani, J.; El-Emam, S.; Wang, H.; Chuang, J.; Kozak, I.; Cheng, L.; Bartsch, D.U.; Freeman, W.R. Choroidal volume variations with age, axial length, and sex in healthy subjects: a three-dimensional analysis. *Ophthalmol.* **2012**, *119*, 2572–2578. [[CrossRef](#)] [[PubMed](#)]
13. Li, Y.; Miara, H.; Ouyang, P.; Jiang, B. The Comparison of Regional RNFL and Fundus Vasculature by OCTA in Chinese Myopia Population. *J. Ophthalmol.* **2018**, *2018*, 3490962. [[CrossRef](#)] [[PubMed](#)]
14. Ratheesh, K.M.; Seah, L.K.; Murukeshan, V.M. Spectral phase-based automatic calibration scheme for swept source-based optical coherence tomography systems. *Phys. Med. Biol.* **2016**, *61*, 7652–7663. [[CrossRef](#)] [[PubMed](#)]
15. Tan, C.S.; Ouyang, Y.; Ruiz, H.; Sadda, S.R. Diurnal Variation of Choroidal Thickness in Normal, Healthy Subjects Measured by Spectral Domain Optical Coherence Tomography. *Investig. Ophthalmol. Vis. Sci.* **2012**, *53*, 261–266. [[CrossRef](#)] [[PubMed](#)]
16. Chhablani, J.; Barteselli, G.; Wang, H.; El-Emam, S.; Kozak, I.; Doede, A.L.; Bartsch, D.U.; Cheng, L.; Freeman, W.R. Repeatability and reproducibility of manual choroidal volume measurements using enhanced depth imaging optical coherence tomography. *Investig. Ophthalmol. Vis. Sci.* **2012**, *53*, 2274–2280. [[CrossRef](#)]
17. Pillebout, E.; Sunderkötter, C. IgA vasculitis. *Semin. Immunopathol.* **2021**, *43*, 729–738. [[CrossRef](#)] [[PubMed](#)]
18. Tan, K.A.; Gupta, P.; Agarwal, A.; Chhablani, J.; Cheng, C.Y.; Keane, P.A.; Agrawal, R. State of science: Choroidal thickness and systemic health. *Surv. Ophthalmol.* **2016**, *61*, 566–581. [[CrossRef](#)]
19. Inoue, R.; Sawa, M.; Tsujikawa, M.; Gomi, F. Association between the efficacy of photodynamic therapy and indocyanine green angiography findings for central serous chorioretinopathy. *Am. J. Ophthalmol.* **2010**, *149*, 441–446.e2. [[CrossRef](#)]
20. Laviers, H.; Zambarakji, H. Enhanced depth imaging-OCT of the choroid: a review of the current literature. *Graefes. Arch. Clin. Exp. Ophthalmol.* **2014**, *252*, 1871–1883. [[CrossRef](#)]

21. Deuter, C.M.; Kötter, I.; Wallace, G.R.; Murray, P.I.; Stübiger, N.; Zierhut, M. Behçet's Disease: Ocular Effects and Treatment. *Prog. Retin. Eye Res.* **2008**, *27*, 111–136. [[CrossRef](#)] [[PubMed](#)]
22. Evereklioglu, C. Current Concepts in the Etiology and Treatment of Behçet Disease. *Surv. Ophthalmol.* **2005**, *50*, 297–350. [[CrossRef](#)] [[PubMed](#)]
23. Aristodemou, P.; Stanford, M. Therapy insight: The Recognition and Treatment of Retinal Manifestations of Systemic Vasculitis. *Nat. Clin. Pract. Rheumatol.* **2006**, *2*, 443–451. [[CrossRef](#)] [[PubMed](#)]
24. Shiari, R.; Jari, M.; Karimi, S.; Salehpour, O.; Rahmani, K.; Yeganeh, M.H.; Parvaneh, V.J.; Hajian, S.; Ghasemi, L.; Safi, S. Relationship between Ocular Involvement and Clinical Manifestations, Laboratory Findings, and Coronary Artery Dilatation in Kawasaki Disease. *Eye* **2020**, *34*, 1883–1887. [[CrossRef](#)]
25. De Andrade, F.A.; Balbi, G.M.; de Azevedo, L.G.B.; Sá, G.P.; Junior, H.V.M.; Klumb, E.M.; Levy, R.A. Neuro-Ophthalmologic Manifestations in Systemic Lupus Erythematosus. *Lupus* **2017**, *26*, 522–528. [[CrossRef](#)]
26. Chuah, J.; Meaney, T. Anterior Ischaemic Optic Neuropathy Secondary to Henoch–Schönlein Purpura. *Eye* **2005**, *19*, 1028. [[CrossRef](#)]
27. Chung, Y.R.; Cho, E.H.; Jang, S.; Lee, S.Y.; Lee, E.S.; Lee, K. Choroidal Thickness Indicates Subclinical Ocular and Systemic Inflammation in Eyes with Behçet Disease without Active Inflammation. *Korean J. Ophthalmol.* **2018**, *32*, 290–295. [[CrossRef](#)]
28. Tetikoglu, M.; Temizturk, F.; Sagdik, H.M.; Aktas, S.; Ozcura, F.; Ozkan, Y.; Temizturk, S. Evaluation of the Choroid, Fovea, and Retinal Nerve Fiber Layer in Patients with Rheumatoid Arthritis. *Ocul. Immunol. Inflamm.* **2017**, *25*, 210–214. [[CrossRef](#)]
29. Kirin, M.; Nagy, R.; MacGillivray, T.J.; Polašek, O.; Hayward, C.; Rudan, I.; Campbell, H.; Wild, S.; Wright, A.F.; Wilson, J.F.; et al. Determinants of retinal microvascular features and their relationships in two European populations. *J. Hypertens.* **2017**, *35*, 1646–1659. [[CrossRef](#)] [[PubMed](#)]
30. Arnould, L.; Seydou, A.; Gabrielle, P.H.; Guenancia, C.; Tzourio, C.; Bourredjem, A.; El Alami, Y.; Daien, V.; Binquet, C.; Bron, A.M.; et al. Subfoveal Choroidal Thickness, Cardiovascular History, and Risk Factors in the Elderly: The Montrachet Study. *Investig. Ophthalmol. Vis. Sci.* **2019**, *60*, 2431–2437. [[CrossRef](#)]
31. Liu, G.Y.; Utset, T.O.; Bernard, J.T. Retinal nerve fiber layer and macular thinning in systemic lupus erythematosus: an optical coherence tomography study comparing SLE and neuropsychiatric SLE. *Lupus.* **2015**, *24*, 1169–1176. [[CrossRef](#)]
32. Bayram, N.; Gundogan, M.; Ozsaygılı, C.; Adelman, R.A. Posterior ocular structural and vascular alterations in severe COVID-19 patients. *Graefes. Arch. Clin. Exp. Ophthalmol.* **2022**, *260*, 993–1004. [[CrossRef](#)] [[PubMed](#)]
33. Arnould, L.; Guillemin, M.; Seydou, A.; Gabrielle, P.H.; Bourredjem, A.; Kawasaki, R.; Binquet, C.; Bron, A.M.; Creuzot-Garcher, C. Association between the retinal vascular network and retinal nerve fiber layer in the elderly: The Montrachet study. *PLoS ONE* **2020**, *15*, e0241055. [[CrossRef](#)] [[PubMed](#)]